Resonant Brillouin scattering by amplified phonons in CdS

Koshi Ando and Chihiro Hamaguchi
Department of Electronics, Faculty of Engineering, Osaka University, Suita, Osaka, Japan
(Received 4 November 1974)

Dispersion spectra of the Brillouin scattering cross section are investigated in the range of photon energy 2.0–2.4 eV at room temperature by making use of intense acoustic phonons amplified through the acoustoelectric effect in CdS. We have found a deep and narrow minimum of the scattering cross section at a photon energy of about 2.22 eV and a steep increase near the fundamental absorption edge. These features are explained in terms of resonant enhancement and cancellation based on Loudon's theory. Theoretical calculation by taking into account the exciton effect shows an excellent agreement with experimental data. Scattering of the virtual intermediate states associated with the p-like A, B, and C valence bands was found to give rise to the resonant enhancement. The dominant contribution comes from the scattering process of the exciton of the B state to the A state by the deformation potential C_6 and the recombination of the A state to emit the scattered photons in the present configuration.

I. INTRODUCTION

The resonant enhancement of the Brillouin (Raman) scattering cross sections near the intrinsic absorption edge in semiconductors has recently received considerable attention both theoretically[1–4] and experimentally.[5–9] The resonant behavior for the Brillouin scattering from thermal acoustic phonons (LA phonons along the c axis) was observed by Pine[5] as the fundamental absorption edge of CdS was thermally tuned through the incident radiation at 5145 Å. The result showed a weak resonant enhancement, while such a resonant cancellation as observed in the Raman scattering cross sections[10,11] was not found. The intense phonon beams amplified by acoustoelectric instabilities are very useful to investigate the dispersion spectra of the resonant enhancement near the fundamental absorption edge. This advantage will be readily understood by the following facts. An application of the drift velocity greater than the sound velocity in piezoelectric semiconductors results in selective acoustoelectric amplification of phonon beams traveling in a narrow frequency range near the frequency of maximum gain.[12] The phonon beams usually form a domain 1 mm wide traveling from the cathode to the anode.

Amplified acoustic phonons have an intensity a factor of the order of 10^9 above thermal equilibrium, which is easily achieved in the frequency range 0.2 to 4.0 GHz. The phonon frequency range is most suitable for Brillouin scattering measurements.[13] The intense acoustic phonons provide strong scattering signals and permit the use of a continuous light source dispersed by a conventional monochromator instead of a laser.

Such measurements were first made by Garrod and Bray.[6] They found resonant enhancement and cancellation of Brillouin scattering cross sections near the fundamental absorption edge. Similar behavior was observed in CdS by the present authors[7] and independently by Gelbart and Many.[8] The main features of our experimental results are the following. A steep increase of the scattering cross section close to the absorption edge is found. A deep and narrow minimum in the cross section is observed at photon energy about 2.22 eV. At longer wavelengths, the scattering cross section approaches the nonresonant Brillouin scattering, namely, the usual Brillouin scattering predicted from the Pockels photoelastic effect.

A macroscopic interpretation[6] is that the appropriate photoelastic constant passes through zero while undergoing a reversal in sign (here we have to note that the scattering cross section is proportional to the square of the photoelastic constant). In fact, the dispersion of the piezobirefringence, which yields the photoelastic constants, shows a reversal in sign. (See, for example, the piezobirefringence coefficients Q_{11}-Q_{12} in Ref. 14, which are related to the photoelastic constants P_{11}-P_{12}). The piezobirefringence coefficient appropriate to the present experiment is not obtained due to the large natural birefringence in CdS.

A microscopic theory for resonant Brillouin scattering has been given by Loudon.[1] The theory is based on a third-order time-dependent perturbation in which the incident photon creates a virtual electron-hole pair, the electron or hole is then scattered by a phonon, and finally, the electron and the hole recombine to emit the scattered photon. In order to explain the cancellation in the Raman scattering, Ralston *et al.*[10] proposed that the scattering amplitude is given by a sum of the resonant and nonresonant terms of opposite sign. The resonant term is given by Loudon's expression and the nonresonant term is interpreted as the contribution of all higher interband excitations of intermediate states. Such analyses are successful in explaining

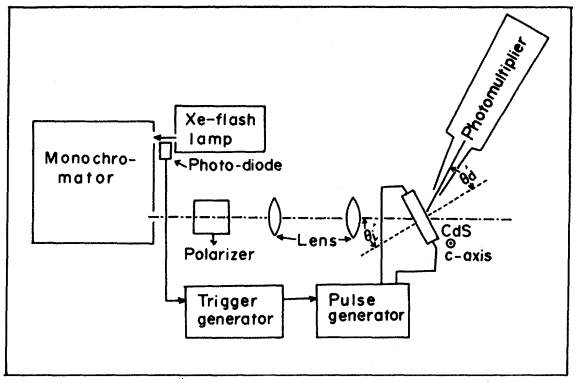

FIG. 1. Schematic diagram of the experimental apparatus. The specimen was mounted on a rotatable table and the incident angle θ_i and the scattered angle $\theta_s (= \theta_i + \theta_d)$ were set to detect light scattered by phonons with a specific frequency.

the resonant Raman scattering in CdS. An analogous treatment was performed to explain the dispersion of the Brillouin scattering cross sections in CdS by Gelbart and Many.[8] They found that a best fit was obtained by a least-square method with the energy gap $E_g = 2.41$ eV, which is smaller than the value obtained by reflectance measurements (2.53 eV). Loudon's theory assumes that the virtual intermediate states are free-electron–hole pairs, and disregards the Coulomb interaction between the electrons and the holes. Modification was made to incorporate the Coulomb interaction by taking into account the virtual intermediate states of the excitons.[2] The latter theory seems to explain the small band gap obtained by Gelbart and Many.

In this paper we report a study of the dispersion spectra of the Brillouin scattering cross section obtained by making use of intense acoustic-phonon beams. We compare the data with the theory of Loudon and also with that of Ganguly and Birman[2] which assumed that the virtual intermediate states are the exciton states, including bound and continuum states. The latter theory gives an excellent agreement with the experimental data. In addition we discuss the interaction between the acoustic shear waves and excited virtual electron–hole pairs by using the orbital-strain Hamiltonian in wurtzite.[15]

II. EXPERIMENTAL PROCEDURES

The experimental arrangement used in the present work is shown schematically in Fig. 1. A high intensity light source of a continuous spectrum was obtained from a xenon flash tube (Ushio Type 626 Xe flash lamp) and dispersed by a monochromator (JASCO CT-50). The resolution was about 5–10 Å in the range of the present experiment. The output beam from the monochromator was focussed onto the CdS sample with incident angle θ_i after passing a polarizer (Gran-Thompson prism) and lenses. The size of the light spot was about 0.5 mm in diameter. High voltage pulses were synchronized with the flash light so as to traverse the acousto-electric domain at the illuminated part of the specimen, and thus the light scattered in the direction $\theta_s = \theta_i + \theta_d$ during the passage of the domain was detected by the photomultiplier. An analyzer (polaroid) was mounted in front of the photomultiplier. The incident angle θ_i and scattered angle θ_d for a given frequency of acoustic phonons were calculated as a function of the incident light wavelength by taking into account the birefringence of the refractive indices. The dimensions of the CdS sample ($n = 2\times10^{15}$ cm^{-3}, $\mu = 285$ cm^2/V sec) used in the experiments were $0.92\times0.16\times0.10$ cm with its long dimension perpendicular to the c axis. The surfaces were polished mechanically and the electrodes were soldered to the indium evaporated end surface. The light beam was incident on a polished surface parallel to the c axis and the scattering plane was perpendicular to the c axis. The polarization directions of the incident and scattered light are parallel and perpendicular to the c axis, respectively. We found that the frequency of maximum intensity was around 2.8 GHz in CdS at the initial stage of the amplification and subsequently the maximum acoustic intensities shifted down to the lower frequencies through parametric down conversion. We measured Brillouin scattering signals for 2, 1, and 0.5 GHz in the present experiments.

III. DETERMINATION OF APPROPRIATE PHOTOELASTIC CONSTANT

In this section we present a macroscopic treatment of Brillouin scattering to deduce the photoelastic constants appropriate to the present experiment, because the resonant enhancement and cancellation of the Brillouin scattering cross section are explained phenomenologically in terms of the wavelength dependence and sign reversal of the photoelastic constant.

The Brillouin scattering cross sections in CdS have been derived by Hope[16] and by one of the authors (C. H.).[13] In the analysis the indirect photoelastic effect due to the piezoelectricity[3,17,18] and also the rotation effect[17,18] are neglected. In this paper we include the indirect effect because the acoustic shear waves are piezoelectrically active (hereafter denoted $T2$-mode acoustic waves). We can neglect the rotation effect because it is found to be quite small in CdS.[13] From the macroscopic theory we obtain for the scattering cross section per unit optical length per unit solid angle

$$\sigma_B = \frac{\pi^2 n_0^8}{\lambda_0^4} \frac{k_B T}{2} \frac{|\xi^\mu|^2}{\rho v_\mu^2} \frac{\cos^2\theta_d}{n_i (n_d^2 - \sin^2\theta_d)^{1/2}} \beta \ , \quad (3.1)$$

where

$$\xi^{\mu}=\frac{n_e^2}{n_0^2}\left[P_{44}+(P_{44})_{\mathrm{ind}}\right]\left[1-\frac{1}{4n_0^2}\frac{\lambda_0^2}{v_\mu^2 f_s^2}\times\left(f_s^2+\frac{v_\mu^2}{\lambda_0^2}(n_0^2-n_e^2)\right)^2\right]^{1/2} \quad (3.2)$$

for the scattering by the piezoelectrically active shear waves traveling in the c-plane with the atomic displacement parallel to the c axis.[15,19,20] In Eqs. (3.1) and (3.2), n_0, n_e and n_d are the refractive indices of ordinary, extraordinary and scattered waves, λ_0 is the incident light wavelength, v_μ and f_s are the sound velocity and frequency of the acoustic waves, and β is the correction factor for the boundary effect.[13,15,19] We find in Eqs. (3.1) and (3.2) that the scattering cross section is proportional to the square of the photoelastic constant $[P_{44}+(P_{44})_{\mathrm{ind}}]$, where P_{44} is the Pockels photoelastic constant and $(P_{44})_{\mathrm{ind}}$ is the indirect photoelastic constant due to the piezoelectricity which is given by[15,19]

$$(P_{44})_{\mathrm{ind}}=-e_{15}r_{51}/\epsilon_{11}\ , \quad (3.3)$$

where e_{15}, r_{51}, and ϵ_{11} are the piezoelectric constant, Pockels electro-optic constant, and dielectric constant, respectively. We find that $(P_{44})_{\mathrm{ind}}$ is about 18% of the Pockels photoelastic constant. This indirect photoelastic effect in macroscopic theory corresponds to the scattering of the intermediate state by the piezoelectric scattering in the microscopic theory. The vector ξ^{μ} determines the polarization vector of the scattered light, and we find that the polarization of the light scattered by the shear waves is rotated by 90° with respect to the incident light polarization when the scattering plane is perpendicular to the c axis. Therefore, the Brillouin scattering signal is easily distinguishable from any background. The configuration of the incident and scattered light polarization is essential to the analysis based on the microscopic theory, because we have to take into account the well known selection rule in CdS. This analysis will be given in Sec. IV.

We find in Eq. (3.1) that the scattering cross section has small dependence of the incident wavelength λ_0. However, this macroscopic treatment cannot explain our experimental dispersion curve of the Brillouin scattering cross section near the absorption edge without assuming wavelength-dependent photoelastic constants.

IV. RESULTS AND DISCUSSION

A. Scattering cross sections

The Brillouin scattering intensities were measured as a function of the incident light wavelength. The results for the piezoelectrically active shear waves of frequencies 0.5, 1.0, and 2.0 GHz are shown in Fig. 2, where the ratio of the scattered intensity I_s to the incident light intensity I_0 is used. The general features are similar to the results of n-GaAs (Ref. 6) if we take into account the strong absorption of the incident and scattered light near the fundamental absorption edge. The scattering efficiency has a narrow and sharp minimum at about 5620 Å. The decrease of the scattering efficiency near the band edge is caused by the strong absorption of the incident and scattered light due to the increase in the absorption coefficient. In order to deduce the Brillouin scattering cross section from the data of I_s/I_0, we have to take into account not only the absorption of the incident and scattered light but also depletion of the light from the various Brillouin components. This was made in GaAs by Garrod and Bray,[6] making use of the normalization of the scattering signal I_s by the transmitted light intensity I_t. They found in an isotropic material like GaAs

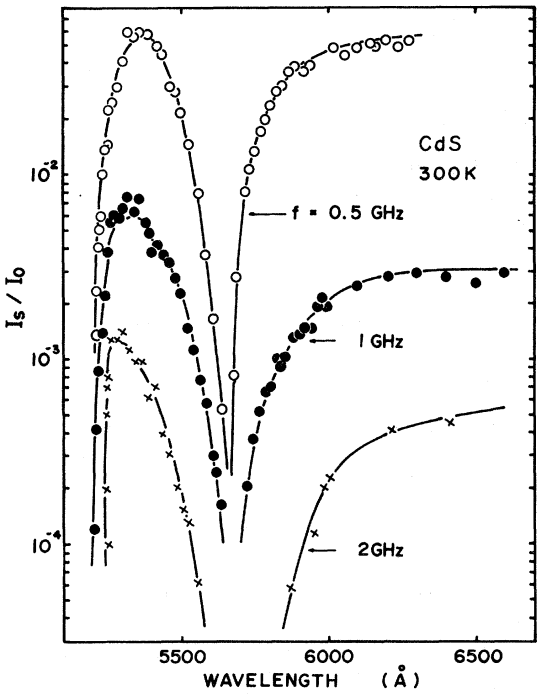

FIG. 2. Brillouin scattering signal in CdS. The ratios of the Brillouin scattered light intensity I_s to the incident light intensity I_0 are plotted as a function of incident wavelength for 0.5-, 1.0-, and 2.0-GHz acoustic phonons.

$$I_s/I_t=\sigma_B b' d\Omega_s\ , \quad (4.1)$$

where b' is the light path length and $d\Omega_s$ is the solid angle in which the light is scattered. Such a relation is not valid in the case of CdS.

The band structure of CdS at $k=0$ consists of a Γ_7 conduction band followed by, in order (the energy gap and then) a top Γ_9 valence band and two lower Γ_7 valence bands.[21] The three valence bands com-

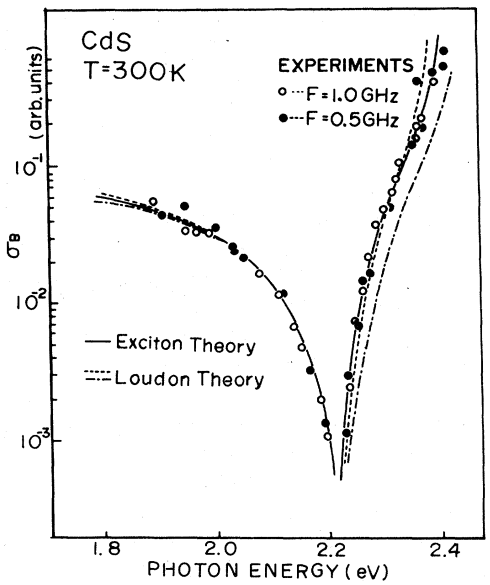

FIG. 3. Dispersion curves of Brillouin scattering cross section for 0.5- and 1.0-GHz acoustic phonons (in arbitrary units). Solid curves were calculated by taking into account the exciton effects with optical band gap; $E_{gi}=2.494$ eV for the incident light and optical band gap; $E_{gs}=2.480$ eV for the scattered light. Dotted and dashed-dotted curves were estimated by Loudon's theory with optical energy gaps; $E_{gi}=2.40$ eV, $E_{gs}=2.38$ eV, and with $E_{gi}=2.494$ eV, $E_{gs}=2.480$ eV, respectively.

pletely split. In the case of incident light polarization parallel to the c axis, the dipole transitions are forbidden between the conduction band and the Γ_9 valence band and allowed between the conduction band and the Γ_7 valence bands. On the other hand, in the case of the polarization perpendicular to the c axis, the transitions between the conduction band and the three valence bands are all allowed. This well known selection rule explains the difference in the optical absorption coefficients for the two different light polarizations observed by Dutton.[22] As shown in the Appendix, a simple analysis which takes into account the difference in the absorption coefficients gives the relation near the fundamental absorption edge

$$\frac{I_s}{I_0}=\frac{\sigma_B d\Omega_s}{\alpha_i-\alpha_d n_d/n_i}\exp\left(-\frac{\alpha_d b}{\cos\theta_d'}\right)\times\left\{1-\exp\left[-\left(\alpha_i-\alpha_d\frac{n_d}{n_i}\right)\frac{b}{\cos\theta_i'}\right]\right\}, \quad (4.2)$$

where α_i and α_d are the absorption coefficients for the incident and scattered light, respectively, and b is the width of the sample in the scattering plane. The refractive indices n_i and n_d refer to the values of the incident and scattered light, and the incident angle θ_i' and the scattered angle θ_d' ($=\theta_s'-\theta_i'$) are defined in Ref. 13. At longer wavelength far from the band edge the values of α_i and α_d are so small that we can approximate Eq. (4.2) by (see the Appendix)

$$\frac{I_s}{I_0}=\frac{\sigma_B b}{\cos\theta_i'}\exp\left(-\frac{\alpha_d+\sigma_T}{\cos\theta_d'}b\right)d\Omega_s\ , \quad (4.3)$$

where σ_T is the total scattering coefficient defined in the Appendix. It is evident that Eq. (4.3) is equivalent to Eq. (4.1). Note that Eq. (4.1) is derived by assuming equal optical path lengths for the scattered and unscattered light; $b/\cos\theta_i'=b/\cos\theta_d'=b'$. Near the band edge, however, the condition $(\alpha_i-\alpha_d n_d/n_i)b\ll 1$ is not satisfied and thus we have to use the expression Eq. (4.2) in order to compute the Brillouin scattering cross section from Fig. 2. By making use of the absorption coefficient data of Dutton[22] and the refractive index data of Bieniewski and Czyzak[23] we calculated the dispersion of the scattering cross section, which is shown in Fig. 3. The magnitude of the scattering cross section is proportional to the energy density of the amplified phonons and thus depends on the applied electric field. Therefore we plotted the results in arbitrary units in Fig. 3. The general features of the dispersion for 0.5-, 1.0-, and 2.0-GHz phonons are quite similar. We find that in the long-wavelength region the scattering cross sections approach to the nonresonant Brillouin scattering, namely, Brillouin scattering cross sections predicted from the photoelastic effect of macroscopic theory.

The wavelength dependence λ_0^{-4} is not found in the present results because of the narrow wavelength range of the incident photons. We find a deep and narrow minimum at 2.22 eV and a steep increase in the higher photon energy region beyond the minimum. These data indicate an existence of the resonant enhancement and cancellation near the fundamental absorption edge in CdS. Therefore, it seems to be most reasonable to expect that the photoelastic constant P_{44} in CdS actually crosses over the zero line at a photon energy of 2.22 eV. The behavior of $(P_{44})_{\rm ind}$ does not play an important role in the above analysis because of the reason discussed later. We discuss here the dispersion spectra of the Brillouin scattering cross section by using the microscopic theory. First we use Loudon's theory without exciton effects and second we extend their analysis to include the exciton effect. The scattering cross section derived by Loudon has the form

$$\sigma_B=\left(\frac{e}{\hbar mc}\right)^4\frac{k_B T}{2\rho v_j^2}\frac{\omega_s}{\omega_i}|R_{is}|^2\ , \quad (4.4)$$

where the most dominant term of R_{is} is given by

$$R_{is}=\frac{1}{V}\sum_{\alpha\beta}\frac{P^2_{0\beta}\Xi_{\beta\alpha}P^1_{\alpha 0}}{(\omega_\beta-\omega_s)(\omega_\alpha-\omega_i)}\ , \quad \omega_s=\omega_i\pm\omega_q\ . \quad (4.5)$$

Here $\hbar\omega_\alpha$ and $\hbar\omega_\beta$ are the energies of the virtual

states, ω_i and ω_s are the angular frequencies of the incident and scattered photons, ω_q is the phonon frequency of wave vector q appropriate to the scattering, $\Xi_{\beta\alpha}$ is the matrix element of deformation potential scattering, and $P_{0\beta}$ and $P_{\alpha 0}$ are the appropriate momentum matrix elements, where subscript 0 stands for the ground state and subscript α and β for the pair states. The superscripts 1 and 2 of the momentum matrix elements indicate their components in the polarization directions of incident and scattered photons. Taking into account the difference in the optical band gaps for the two different light polarizations in CdS, we obtain for the spherical and parabolic bands[24]

$$R_{is} = \frac{2}{(2\pi)^2}\sum_{\alpha\beta}\left(\frac{2\mu}{\hbar}\right)^{3/2}\frac{P^2_{0\beta}\Xi_{\beta\alpha}P^1_{\alpha 0}}{\omega_{g\beta}-\omega_{g\alpha}+\omega_q} \times\left[(\omega_{g\beta}-\omega_s)^{1/2}\arctan\left(\frac{\Delta\omega_\beta}{\omega_{g\beta}-\omega_s}\right)^{1/2} -(\omega_{g\alpha}-\omega_i)^{1/2}\arctan\left(\frac{\Delta\omega_\alpha}{\omega_{g\alpha}-\omega_i}\right)^{1/2}\right], \quad (4.6)$$

where μ is the reduced mass, which is assumed to be equal for the α and β pair states for simplicity, $\hbar\omega_{g\alpha}$ and $\hbar\omega_{g\beta}$ are the optical band gaps for the pair states α and β corresponding to the incident and scattered light, respectively, and $\hbar\Delta\omega_\alpha$ (or $\hbar\Delta\omega_\beta$) is the combined width of the conduction and valence bands. Equations (4.5) and (4.6) indicate that the scattering cross sections increase as the incident photon energy $\hbar\omega_i$ approaches the band gap $\hbar\omega_{g\alpha}$ or $\hbar\omega_{g\beta}$. This results in a resonant Brillouin scattering.

The cancellation is explained by assuming that the resonant contribution (R_{is}) to the scattering efficiency is opposite in sign to the nonresonant contribution ($-R_0$) arising from other, far-off critical points in the band structure. In other words the scattering cross section is given by

$$\sigma_B \propto |R_{is}-R_0|^2 . \quad (4.7)$$

Without the knowledge of the matrix elements $P_{0\beta}$, $P_{\alpha 0}$, and $\Xi_{\beta\alpha}$ we can fit experimental data with the use of Eq. (4.7). Later we calculate the matrix element $\Xi_{\beta\alpha}$ by taking into account the three valence bands. It will be shown in Sec. IV B that the dominant contribution to R_{is} is the transition between the B and A valence bands through the deformation potential matrix element Ξ_{AB}. From the present experimental conditions we find that $\hbar\omega_{g\alpha}(\hbar\omega_{g\beta})$ is the energy gap between the B (A) valence band and the conduction band. Using Eqs. (4.6) and (4.7) we calculated the total scattering cross section for the $T2$ mode phonons. In our calculation we used values of $\hbar\Delta\omega_\alpha$ (or $\hbar\Delta\omega_\beta$) in the range of 0.1–10 eV and we found that the results are weakly dependent on the values. We adjusted the value R_0 and energy gaps to fit the experimental curve. We found that the calculated curve fitted the experimental data when we used $\hbar\omega_{g\alpha}=2.40$ eV and $\hbar\omega_{g\beta}=2.38$ eV. The results are shown in Fig. 3 by the dotted curve. Similar analysis was made by Gelbart and Many,[8] who found that the best fit to the data was obtained by using the energy gap $\hbar\omega_{g\alpha}=2.41$ eV, which is in good agreement with the present result. It should be noted that they plotted I_s/I_t as a function of incident photon energy and that such a plot does not give correct values of σ_B near the band edge due to the reason stated earlier. The energy gap obtained in the above analysis is much smaller than the value 2.53 eV deduced from reflectance measurements by Cardona and Harbeke.[25] The values of energy gaps are also estimated from electroreflectance data made by Cardona *et al.*,[26] who found peaks in the electroreflectance spectra at 2.452, 2.466, and 2.525 eV. If we take into account the exciton effects by using the theory of Blossey[27] we have higher-energy gaps by exciton binding energy (28 meV) than the peak values obtained by Cardona *et al.*[26] (See Fig. 8 of Ref. 7); therefore, we obtain $\hbar\omega_{gA}=2.480$ eV, $\hbar\omega_{gB}=2.494$ eV, and $\hbar\omega_{gC}=2.553$ eV. Absorption coefficients at $\hbar\omega_{g\alpha}=2.4$ eV and $\hbar\omega_{g\beta}=2.38$ eV are estimated from Dutton's data to be about 10^2 cm^{-1}. Such large values at photon energies lower than the band gaps can be explained by the exciton effect.

As we mentioned in Sec. I, the Coulomb interaction is always present between the excited electrons and holes, and thus it seems to be reasonable to assume that the virtual intermediate states are the exciton states. Loudon's formulation has been modified by Ganguly and Birman[2] to include the exciton effects. After simple manipulation we find[31]

$$R_{is} = \sum\frac{P^2_{0\beta}\Xi_{\beta\alpha}P^1_{\alpha 0}}{\omega_{g\beta}-\omega_{g\alpha}+\omega_q}\left(\frac{1}{\pi a_0^{*3}}\sum_n\frac{1}{n^3}\left(\frac{1}{(\omega_{g\alpha}-R^*/n^2-\omega_i)(\omega_{g\beta}-R^*/n^2-\omega_s)}\right)+\frac{1}{4\pi\omega_q}\left(\frac{2\mu}{\hbar}\right)^{3/2}(4\pi^2R^*)^{1/2}\right) \times\left\{\left[1-\exp\left(-\frac{4\pi^2R^*}{\omega_{g\beta}-\omega_s}\right)^{1/2}\right]^{-1}-\left[1-\exp\left(-\frac{4\pi^2R^*}{\omega_{g\alpha}-\omega_i}\right)^{1/2}\right]^{-1}\right\}, \quad (4.8)$$

where $a_0^*=\epsilon\hbar^2/\mu e^2$ is the exciton Bohr radius and $\hbar R^*=\mu e^4/2\hbar^2\epsilon^2$ is the exciton rydberg constant. In Eq. (4.8) the first term corresponds to the discrete levels and the second term corresponds to the con-

tinuum electron-hole pair states. As it is well known, the three valence bands labeled A, B, and C in conjunction with the Γ_7 conduction band gives rise to A, B, and C series of exciton states, respectively. The selection rule for the momentum matrix element is the same as that of the band-to-band transition. We take into account the A and B exciton states for the virtual intermediate states because the dominant contribution to the resonant enhancement comes from the bands with the band gap close to the incident or scattered photon energy. We present here a calculation of the total scattering cross section by using an energy gap of 2.480 eV for the A state and 2.494 eV for the B state. The exciton binding energy is reported to be 28 meV in CdS and we used this value for both states. In the calculation we used the values of oscillator strengths reported by Thomas and Hopfield.[28] The only adjustable parameter was R_0 which was chosen to give a minimum scattering cross section at 2.22 eV. The calculated result is shown by the solid curve in Fig. 3, where we find a better and excellent agreement with the experimental results in the whole range of the present investigation.

It should be noted here that there exist a dc electric field ($\sim 5\times10^3$ V/cm) and an ac field ($\sim 10^4$ V/cm) associated with the piezoelectric potential in the acoustoelectric domain. When the electric fields are capable of ionizing the exciton, the analysis made here is not correct. However, we find that the ionization field of the exciton in CdS is about[27] 1.4×10^5 V/cm which is much higher than the dc or ac field associated with the acoustoelectric domain. Thus we can conclude that the electric fields do not dominate the Coulomb potential and that the present treatment is adequate.

B. Matrix element for the deformation-potential scattering

In Sec. IV A, we assumed that piezoelectric scattering of conduction electrons does not play an important role in the transition of the virtual states and that the matrix element Ξ_{AB} for the deformation-potential scattering between the B and A states is nonvanishing. We will discuss these assumptions here. The orbital-strain Hamiltonian for the p-like valence bands of wurtzite at $k=0$ is given by[14,29]

$$\begin{aligned} H_{xv} = {} & (C_1 + C_3 L_z^2) e_{zz} + (C_2 + C_4 L_z^2)(e_{yy} + e_{xx}) \\ & + C_5 (L_-^2 e_+ + L_+^2 e_-) \\ & + C_6 ([L_z L_+] e_{-z} + [L_z L_-] e_{+z}) \ , \end{aligned} \tag{4.9}$$

and for the electron in the conduction band by

$$H_{xc} = d_1 e_{zz} + d_2 (e_{xx} + e_{yy}) \ , \tag{4.10}$$

where the coefficients C_i and d_i are deformation potentials, the e_{ij}'s are components of the strain tensor with $e_\pm = e_{xx} - e_{yy} \pm 2ie_{xy}$ and $e_{\pm z} = e_{xz} \pm e_{yz}$, L_i and $L_\pm$ are the standard orbital angular momentum operators, and $[L_i L_j] = \frac{1}{2}(L_i L_j + L_j L_i)$. We find from Eq. (4.10) that deformation potential scattering of electrons in the conduction bands disappears for the $T2$ mode acoustic phonons because the only non-vanishing strain components for the $T2$ mode are $e_{\pm z}$. Piezoelectric potential scattering gives rise to a nonvanishing matrix element for the $T2$ mode.[31] However, Berkowicz and Price[9] reported recently that nonpiezoelectric acoustic shear waves propagating along the c axis result in resonant enhancement and cancellation quite similar to the case of the $T2$ mode phonons. The scattering cross section for shear waves propagating along the c axis is given by Eq. (3.1) with

$$|\xi^\mu| = P_{44}(\epsilon_{33}/\epsilon_{11})(P_{k0})_3 \ , \tag{4.11}$$

with no contribution from the indirect photoelastic effect. Therefore a macroscopic theory indicates that the resonant enhancement and cancellation can be interpreted in terms of the direct photoelastic constant P_{44} only. From these results we conclude that the piezoelectric scattering does not play an important role in the scattering cross section.

In addition it is more important to emphasize that such mechanisms based on the scattering of excited electrons can not explain the difference in the energy gaps between the two light polarizations. In order to explain the difference in the optical band gaps, we have to take into account virtual states in the valence bands. We used the wave functions of the three split valence bands derived by Hopfield,[14,30] and calculated the matrix elements of the transitions of the virtual states associated with the valence bands. We found the following result[31]:

$$\begin{aligned} & \Xi_{AB} = \tfrac{1}{2} a_C C_6 = 0.359 \text{ eV } (-1.08 \text{ eV}), \\ & \Xi_{CB} = -C_6 = -0.8 \text{ eV } (2.4 \text{ eV}) \ , \\ & \Xi_{CA} = -\tfrac{1}{2} a_B C_6 = -0.437 \text{ eV } (1.31 \text{ eV}) \ , \\ & \Xi_{BB} = \Xi_{AA} = \Xi_{CC} = 0 \ , \end{aligned} \tag{4.12}$$

where the admixture coefficients a_B and a_C can be determined from the two parameters of the quasi-cubic model; i.e. the spin-orbit and the trigonal field parameters.[14] The numerical values in Eq. (4.12) were calculated by using $C_6 = 0.80$ eV,[29] and the values in parentheses were estimated from $C_6 = -2.4$ eV.[32] The selection rules of both the momentum matrix elements and deformation potential matrix elements are consistent with the experimental condition of our work and with the existence of the two band gaps for the two different light polarizations in CdS, as follows. The incident photons are polarized along the c axis and the excitation of virtual B and C excitons (or excitation of holes in B and C valence bands) are allowed. We can ignore the contribution from the C band for the reason of a large energy separation. Therefore the excited

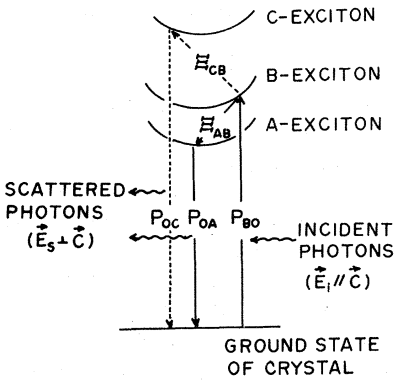

FIG. 4. Schematic diagram of deformation potential scattering of virtual B exciton by acoustic phonons, where $E_{\beta\alpha}$ is the matrix element for the deformation potential scattering from the α state to the β state and $P_{\alpha 0}$ is the momentum matrix elements. (Suffix 0 indicates the ground state.) The polarization vectors for the incident and the scattered light are indicated by $\vec{E}_i$ and $\vec{E}_s$, respectively. The solid line indicates a dominant contribution and the dotted line a weak contribution to the resonant Brillouin scattering. Excitation of the C exciton is not shown to avoid complexity.

holes in the B valence band are scattered by the deformation potential C_6 to the A valence band, where the corresponding matrix element is Ξ_{AB}. The holes in the A band recombine with the excited electrons in the conduction band to emit photons of polarization perpendicular to the c axis. (This transition is allowed.) A schematic diagram for the present experimental condition is shown in Fig. 4, where the transitions indicated by solid lines are dominant ones and those of dotted lines are weak. In Fig. 4 we neglected excitations of virtual C excitons because of the large energy separation.

V. CONCLUSION

We have investigated the dispersion spectrum of the Brillouin scattering cross section by making use of intense acoustic phonons of 0.5, 1.0, and 2.0 GHz amplified through acoustoelectric effect in CdS.

We have found a deep and narrow minimum at the incident photon energy 2.22 eV and a steep increase in the higher photon energy region beyond the minimum. The dispersion spectrum is well explained by taking into account the transition of the virtual states associated with the p-like valence bands and of the exciton effect. It has been shown that the matrix elements for the transition of the virtual states between the B and A valence bands are nonvanishing and yield a dominant contribution to the resonant enhancement. Our analysis shows that the transitions of the excited electrons by both deformation potential and piezoelectric potential do not contribute to the resonant enhancement for the shear acoustic waves investigated in the present experiment. We conclude that the resonant enhancement of the Brillouin scattering in CdS reflects the selection rules for the momentum matrix elements and deformation potential matrix elements.

ACKNOWLEDGMENTS

We are pleased to acknowledge early communication from Professor R. Bray and his critical reading of the manuscript. We would like to thank Prof. H. Hasegawa and Dr. S. Sakoda of Kyoto University for the valuable discussions on the matrix elements for the deformation potential scattering. We also acknowledge the assistance of Dr. M. Yamada in the initial measurements and discussions with Professor J. Nakai and M. San'ya. The present work was supported by the Scientific Research Grant from the Ministry of Education.

APPENDIX

We present here a derivation of the formula to relate the scattering cross section σ_B with the measured values of I_s and I_0, where we properly take into account the birefringence and the difference in the optical absorption coefficients for the incident and scattered light.[33] The light intensity $I(x')$ propagating in the material is expressed by

$$I(x') = I_0 \exp[-(\alpha_i + \sigma_T)x'] \quad , \tag{A1}$$

where I_0 is the incident light intensity, α_i is the absorption coefficient of the incident light, and σ_T is the total Brillouin scattering coefficient.[34,35] The total scattering coefficient σ_T is defined by the relation $I_t = I_t^0 \exp(-\sigma_T b')$, where I_t^0 is the transmitted light in the absence of any scattering, I_t is the light transmitted after depletion by scattering, and b' is the optical path length. The quantity σ_T describes how much light is scattered out of the incident beams by phonons of all possible wave vectors that can contribute to the scattering. The differential scattering intensity $dI_s(x')$ along the optical path between x' and $x'+dx'$ in the material is given by

$$dI_s(x') = I \exp[-(\alpha_i + \sigma_T)x'] \sigma_B \, dx' \, d\Omega_s \quad , \tag{A2}$$

where $d\Omega_s$ is the solid angle determined by the cone angle of the detector.

For the Brillouin scattering in a birefringent material, the angles of incident and scattered light (θ_i' and θ_d', respectively) with respect to the normal to the sample are different in general. When we define a distance x by $x' \cos\theta_i'$, x is the effective optical path length along the direction normal to the surface, and Eq. (A2) reduces to

$$dI_s(x)=I_0\exp\left(\frac{-(\alpha_i+\sigma_T)x}{\cos\theta_i'}\right)\frac{\sigma_B\,dx\,d\Omega_s}{\cos\theta_i'}\ . \qquad \text{(A3)}$$

Light intensity scattered at the point x', is also decreased by absorption and scattering during the path length $x''(=b'-x')$, where $x''\cos\theta_d'=b-x$, and b is the width of the sample in the scattering plane. Therefore, the actual Brillouin scattered light intensity is given by

$$\begin{aligned}dI_s(x,b)&=dI_s(x)\exp[-(\alpha_d+\sigma_T)x'']\\&=I\exp\left\{-\left[\left(\alpha_i-\alpha_d\frac{\cos\theta_i'}{\cos\theta_d'}\right)+\sigma_T\left(1-\frac{\cos\theta_i'}{\cos\theta_d'}\right)\right]\right.\\&\left.\times\frac{x}{\cos\theta_i'}-\frac{(\alpha_d+\sigma_T)b}{\cos\theta_d'}\right\}\frac{\sigma_B\,dx\,d\Omega_s}{\cos\theta_i'}\ , \qquad \text{(A4)}\end{aligned}$$

where α_d is the absorption coefficient of the scattered light. Integrating Eq. (A4) over the sample width, we obtain

$$\begin{aligned}\frac{I_s}{I_0}&=\frac{\sigma_B\,d\Omega_s}{(\alpha_i-\alpha_d n_d/n_i)+\sigma_T(1-n_d/n_i)}\\&\times\exp\left(-\frac{(\alpha_d+\sigma_T)b}{\cos\theta_d'}\right)\times\left(1-\exp\left\{-\left[\left(\alpha_i-\alpha_d\frac{n_d}{n_i}\right)\right.\right.\right.\\&\left.\left.\left.+\sigma_T\left(1-\frac{n_d}{n_i}\right)\right]\frac{b}{\cos\theta_i'}\right\}\right)\ , \qquad \text{(A5)}\end{aligned}$$

where n_i and n_d are the refractive indices for the incident and scattered light, respectively, and we used a relation $n_i\cos\theta_i'=n_d\cos\theta_d'$.

Noting that $|n_d/n_i-1|\ll 1$ and $(\alpha_i-\alpha_d n_d/n_i)\gg\sigma_T(1-n_d/n_i)$ near the absorption edge ($\alpha_d\gg\sigma_T$) we find, from Eq. (A5),

$$\begin{aligned}\frac{I_s}{I_0}&=\frac{\sigma_B\,d\Omega_s}{\alpha_i-\alpha_d n_d/n_i}\exp\left(-\frac{\alpha_d b}{\cos\theta_d'}\right)\\&\times\left\{1-\exp\left[-\left(\alpha_i-\alpha_d\frac{n_d}{n_i}\right)\frac{b}{\cos\theta_i'}\right]\right\}\ . \qquad \text{(A6)}\end{aligned}$$

In the region far from the edge $[(\alpha_i-\alpha_d n_d/n_i)b/\cos\theta_i'\ll 1]$, we obtain

$$\frac{I_s}{I_0}=\sigma_B\,d\Omega_s\,b\exp\left(-\frac{(\alpha_d+\sigma_T)b}{\cos\theta_d'}\right)\Big/\cos\theta_i' \qquad \text{(A7)}$$

or

$$I_s/I_t^d=\sigma_B\,d\Omega_s\,b/\cos\theta_i'\ , \qquad \text{(A8)}$$

where I_t^d is the transmitted beam for the light polarization in the same direction as the scattered light.

[1]R. Loudon, Proc. R. Soc. Lond. A 275, 218 (1963); J. Phys. (Paris) 26, 677 (1965).

[2]A. K. Ganguly and J. L. Birman, Phys. Rev. 162, 806 (1967).

[3]E. Burstein, R. Ito, A. Pinczuk, and M. Shand, J. Acoust. Soc. Am. 49, 1013 (1971).

[4]B. Bendow and J. Birman, Phys. Rev. B 1, 1678 (1970).

[5]A. S. Pine, Phys. Rev. B 5, 3003 (1972).

[6]D. K. Garrod and R. Bray, *Proceedings of the Eleventh International Conference on the Physics of Semiconductors*, Warsaw, 1972 (Polish Scientific, Warsaw, 1973), p. 1167; Phys. Rev. B 6, 1314 (1972).

[7]M. Yamada, K. Ando, C. Hamaguchi, and J. Nakai, J. Phys. Soc. Jpn. 34, 1696 (1973).

[8]U. Gelbart and A. Many, Phys. Lett. A 43, 329 (1973).

[9]R. Berkowicz and D. H. R. Price, Solid State Commun. 14, 195 (1974).

[10]J. M. Ralston, R. L. Wadsack, and R. K. Chang, Phys. Rev. Lett. 25, 814 (1970); see also, *Proceedings of the Second International Conference on Light Scattering in Solids*, edited by M. Balkanski (Flammarion, Paris, 1971).

[11]T. C. Damen and J. F. Scott, Solid State Commun. 9, 383 (1971).

[12]M. Yamada, C. Hamaguchi, K. Matsumoto, and J. Nakai, Phys. Rev. B 7, 2682 (1973); this contains a list of relevant references.

[13]C. Hamaguchi, J. Phys. Soc. Jpn. 35, 832 (1973).

[14]P. Y. Yu and M. Cardona, J. Phys. Chem. Solids 34, 29 (1973).

[15]C. Hamaguchi, K. Ando, M. San'ya and M. Yamada, Symposium on Microwave Acoustics, Lancaster, England, 1974 (unpublished).

[16]L. L. Hope, Phys. Rev. 166, 883 (1968).

[17]D. F. Nelson, P. D. Lazay, and M. Lax, Phys. Rev. B 6, 3109 (1972).

[18]D. F. Nelson and M. Lax, Phys. Rev. B 3, 2778 (1971).

[19]M. San'ya and C. Hamaguchi (unpublished).

[20]In Equation (3.1) we took into account the effect of astigmatism pointed out by M. Lax and D. F. Nelson, in *Proceedings of the Third Rochester Conference on Coherence and Quantum Optics*, edited by L. Mandel and E. Wolf (Plenum, New York, 1973), p. 415. The term $\cos\theta_d/[n_d(n_d^2-\sin^2\theta_d)^{1/2}]$ in the simplified expression of Ref. 13 should be replaced by $\cos\theta_d/[n_i(n_d^2-\sin^2\theta_d)^{1/2}]$ as given in Eq. (3.1). In the present experiment, the collection angle was constant and the change in the inside collection angle in the scattering plane was estimated to be about $\pm 5°$, which gives rise to a slight decrease (5%) in the scattering cross section at the long-wavelength range. Thus we can neglect the effect in the experimental region.

[21]J. L. Birman, Phys. Rev. Lett. 2, 157 (1959).

[22]D. Dutton, Phys. Rev. 112, 785 (1958).

[23]J. M. Bieniewski and S. J. Czyzak, J. Opt. Soc. Am. 53, 496 (1963).

[24]Equation (4.6) can be derived from the result of Pines (Ref. 5) [Eqs. (8a) and (8b) of Ref. 5)] by taking into account two different energy gaps for light polarized parallel and perpendicular to the c axis in CdS. See also Ref. 1.

[25]M. Cardona and G. Harbeke, Phys. Rev. 137, A1467 (1965).

[26]M. Cardona, K. L. Shaklee, and F. H. Pollak, Phys. Rev. 154, 696 (1967).

[27]D. F. Blossey, Phys. Rev. B 3, 1382 (1971).

[28]D. G. Thomas and J. J. Hopfield, Phys. Rev. 116, 573 (1959).

[29]D. W. Langer, R. N. Euwema, K. Era, and T. Koda, Phys. Rev. B 2, 4005 (1970).

[30]J. J. Hopfield, J. Phys. Chem. Solid 15, 97 (1960).
[31]K. Ando and C. Hamaguchi (unpublished).
[32]J. E. Rowe, M. Cardona and F. H. Pollak, in *II-V Semiconducting Compounds*, edited by D. G. Thomas (Benjamin, New York, 1968).
[33]It was pointed out by M. Yamada that the difference in absorption coefficients between the incident and scattered light should be taken into account for the calculation of the scattering intensity near the fundamental absorption edge.
[34]D. L. Spears, Phys. Rev. B 2, 1931 (1970).
[35]E. D. Palik and R. Bray, Phys. Rev. B 3, 3302 (1970).